

Received February 16, 2021, accepted April 6, 2021, date of publication April 16, 2021, date of current version April 27, 2021.

Digital Object Identifier 10.1109/ACCESS.2021.3073754

Forecast of Renewable Curtailment in Distribution Grids Considering Uncertainties

ELENA MEMMEL^{ID}, SUNKE SCHLÜTERS^{ID}, RASMUS VÖLKER^{ID}, FRANK SCHULDT^{ID},
KARSTEN VON MAYDELL, AND CARSTEN AGERT

DLR Institute of Networked Energy Systems, 26129 Oldenburg, Germany

Corresponding author: Elena Memmel (elena.memmel@dlr.de)

ABSTRACT Renewable energies curtailment induced by grid congestions increase due to grown renewable energies integration and the resulting mismatch of grid expansion. Short-term predictions for curtailment can help to increase the efficiency of its management. This paper proposes a novel, holistic approach of a short-term curtailment prediction for distribution grids. The load flow calculations for congestion detection are realized by taking different operational security criteria into account, whereas the models for the node-injections are adjusted to the characteristic of each grid node specifically. The determination of required curtailment based on the resulting congestions considers uncertainties of component loading and its corresponding probability. The forecast model is validated using an actual 110 kV distribution grid located in Germany. In order to meet the requirements of a forecast model designed for operational business, prediction accuracy, and its greatest source of error are analyzed. Furthermore, a suitable length of training data is investigated. Results indicate that a six month time period for maintenance gains the highest accuracy. Curtailment prediction accuracy is better for transmission system operator components than for distribution system operator components, but the Sørensen Dice factor for the aggregated grid shows a high match of historic and predicted curtailment with a value of 0.84 and a low error for curtailed energy, which makes 2.23% of the historic curtailed energy. The model is a promising approach, which can contribute to improvement of curtailment strategies and enable valuable insight into distribution grids.

INDEX TERMS Power system operation, distribution grid, power flow analysis, congestion management, renewable power curtailment, short-term prediction, probabilistic uncertainty quantification.

NOMENCLATURE

ACRONYMS

CDF	cumulative distribution function
CFE	Cornish-Fisher Expansion
DM	distribution mapping
DSO	distribution system operator
HV/EHV	high voltage/extra high voltage
LIFO	last in first out
MAE	mean absolute error
MV	medium voltage
PDF	probability density function
RE	renewables
RV	random variable
TSO	transmission system operator

WP	wind power
WTPF	wind turbine power curve

SYMBOLS

P	real power
ΔP	reduction of real power
I, L	grid nodes
I_j^{\max}	maximal current of component j

SUBSCRIPTS

j	component
-----	-----------

I. INTRODUCTION

A challenge of the energy transition are grid overloads resulting from increasing injections of renewables (RE) into the grid whereby, among other things, the maximum

permissible currents are exceeded. In such cases the grid stability can be maintained by curtailing the RE. But curtailment means a spillage of energy [1]. Staudt *et al.* stated the ability of congestion forecast to reduce the amount of required curtailment [2]. Furthermore mitigation of congestions can be enabled, by a more efficient commitment of flexibility options like energy storage, which can help to decrease the amount of RE curtailment [3], using congestion forecasts.

In Germany those curtailments are regulated by the so called feed-in management (“Einspeisemanagement”) [4] defined by §14 EEG (Erneuerbare Energien Gesetz). It allows the system operator to resolve congestions by curtailment in real time. With a new regulation feed-in management will be transitioned into a new approach called “Redispatch 2.0” until October 2021 [5]. As forecasts of upcoming congestions are mandatory for redispatch [6], system operators will need to make short-term predictions about overloads in the distribution grid and the transformers connected to the transmission grid.

In literature, approaches exist describing the prediction of curtailment for long term scenarios in the context of expansion planning [7]–[10] and during RE integration planning [11] or for congestion management in real time grid operation [12], [13]. Short-term predictions of congestions are essentially required for participants of energy markets in the context of redispatch [2] and locational marginal prices [14]. Staudt *et al.* apply artificial neural networks to predict hourly data transmission congestions [2], whereas Zhou *et al.* proposed an approach combining complex hull techniques and system pattern for transmission congestion and locational marginal prices prediction [14]. To keep the model computational efficient, system simplifications have been made [14].

To predict RE curtailment caused by congestions in distribution grids or at connected high voltage/extra high voltage (HV/EHV) transformers requires detailed information, like grid topology, or node specific injections, and consumption for the grid of interest [15], [16]. Furthermore curtailment can occur for just some minutes wherefore its prediction requires a high temporal resolution. For German DSOs a short-term curtailment prediction is highly required for operational business. However, to the best of our knowledge, such a holistic deterministic approach for short-term curtailment prediction in distribution grids considering uncertainties has not been presented in any existing literature study at the time of writing. Therefore, a novel approach of a short-term prediction model for congestion induced RE curtailment in distribution grids is proposed. In order to gain a higher temporal resolution the prediction is based on quarter hourly meteorological forecast data. The corresponding output of the model is the forecast of which RE power plants need to be curtailed and to which extend. This could be a valuable information for optimizing curtailment by applying flexibility options [16]. The model is designed to be individually adaptable to a specific grid, by adjusting nodes of the high voltage (HV) level to their specific in-feed and consumption applying our previous

work proposed in [17]. Therefore historic power flow data of medium voltage/high voltage (MV/HV) transformers and the grid topology provided by corresponding system operators are applied. Using power flow calculations to detect grid congestions contingencies, dynamic line rating, and uncertainties of component loading are considered. In order to make it applicable for operational business the model is validated for an actual distribution grid and the appropriate time period of available data used for model fitting is analyzed in the context of model maintenance. Also the impact of certain input parameters is discussed, as well as its transferability to different grid regions.

Summing up the main contribution of this paper:

- A novel approach for short-term curtailment prediction in distribution grids considering uncertainties is proposed, meeting the requirements for predictions with a high temporal and spatial resolution defined by upcoming changes like “Redispatch 2.0”.
- The approach is adaptable to a specific grid and is designed to be transferable to other grids.
- The prediction model is validated and impacts of certain parameters like wind speed and the appropriate time period of data sets used for model configuration are analyzed.

This paper is organized as follows: The model is described in Section II and in Section III the results of the validation and prediction of a real distribution grid are shown. In Section IV the results are discussed and in V concluded.

II. MODEL DESCRIPTION

A. THEORETICAL BACKGROUND

In order to predict curtailment, the congested components have to be determined. This requires load flow simulations, or analytic approaches, derived from load flow, as realized in [18]. Time series of generation and consumption at the nodes are simulated either probabilistic [9], or deterministic [11].

A vital element here is the definition of a congested line or transformer. If the thermal threshold of a component is exceeded this component is congested. This threshold is, considering lines, effected by dynamic line rating [10]. In addition contingencies in the context of N-1 security have to be considered [9], [10] for lines and transformers. So both aspects have to be implemented in a congestion forecast [9].

In cases of congested components, the generation units, that need to be curtailed, and the required power reduction have to be determined. Therefore sensitivity factors, as used in [9], [18], describing the interrelation between injection nodes and congested components, are utilized.

Furthermore, several approaches exist for selecting the REs for curtailment and determining the amount of power reduction: in the context of planning new RE units the so called “Last in First Out” (LIFO) approach is a commonly used approach [11]. Another option is to optimize the curtailment regarding the overall amount of curtailed power by applying

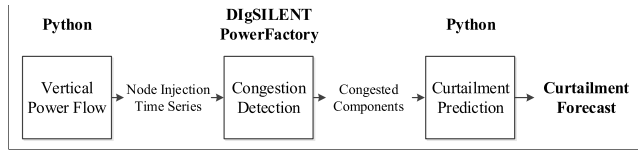


FIGURE 1. Overview of the whole approach consisting of the vertical power flow (described in subsection B1) the congestion detection (described in subsection B2) and the curtailment prediction (described in subsection B3).

mixed integer programming technique to select wind parks and the corresponding power reduction considering all congested components simultaneously [13].

In Germany a congestion is resolved by an iterative reduction of the RE in-feed, which shows the highest sensitivity to the current congested component [19]. Due to the applied communication technology this is realized in four levels: 100% of the available power, and 60%, 30%, and 0% in-feed of the installed capacity [20]. In such cases the system has to remain stable, the curtailed energy has to be sufficiently low and the units to be curtailed are chosen non-discriminatory [20].

Integrating forecast into an operation system with a high share of RE requires information about its uncertainty [21], [22]. If historical values are available probabilistic approaches can be used to determine the uncertainty of an power flow [23]. Such methods are often applied in probabilistic load flow as in [24]–[26]. The objective is to determine the probability density function (PDF) of the uncertain input parameters and its corresponding outputs, that are treated as random variables (RVs) [23]. The error of component loading can be described by its marginal RVs: the error of the node injections. In cases of such multivariate RVs a convolution would become necessary in order to determine the corresponding PDF using the marginals RVs. A common alternative is to use cumulants instead, combined with an arithmetic process [23] like Gram-Charlier [23], Cornish-Fisher Expansion (CFE), as used in [25], or Edgeworth series, as applied in [27].

B. CURTAILMENT FORECAST

The proposed short-term forecast model for RE curtailment in distribution grids consists of two components: the curtailment forecast and the quantification of the uncertainty of the component loading. Both parts are described in the following.

The model can be separated into three parts illustrated in Fig. 1: the calculation of the node-injections, the detection of congestions in the 110 kV distribution grid and the determination of required curtailment.

The node injections are calculated corresponding to our previous work [17]. The applied load profiles and functions describing the RE generation are adjusted individually to each node. In cases of wind farms directly connected to the HV grid level no measured power was available, therefore the wind power is calculated by applying a general wind turbine power curve and site specific wind speeds. In order to predict

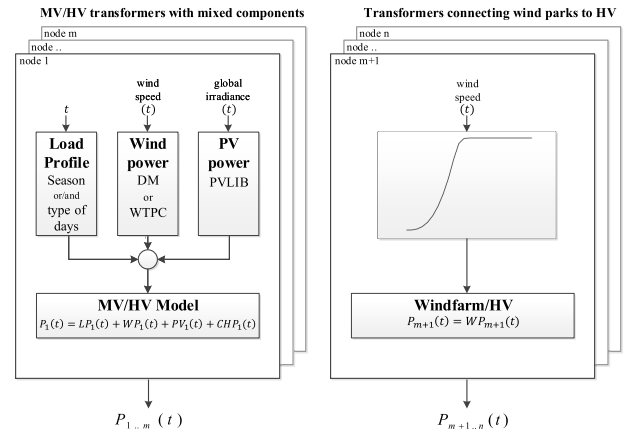


FIGURE 2. Description of the model determining the vertical power flow on MV/HV transformers (left) and windparks directly connected to the HV grid (right).

possible congestions, load flow calculations are performed in DIGSILENT PowerFactory using a HV distribution grid model, provided by the grid operator in charge. Dynamic line rating and contingencies are taken into account. The determination of curtailment is carried out on basis of the resulting bottlenecks. Starting with the most sensitive node the curtailment level is increased until the grid congestion is resolved.

1) MODELING OF THE NODE INJECTIONS

The specific injection of each node connected to MV/HV transformers are represented by the model for the vertical power flow on MV/HV transformers according to our previous paper [17] visualized in Fig. 2. The power flow for one time step is determined by the aggregated power of available consumption and generation separately for each node. Two methods have been applied to represent the node specific infeed of all connected wind farms: the so called *distribution mapping* (DM) approach, introduced in [28] and a five parameter logistic function [29] applied as a representation for the wind turbine power curve (WTPC).

In order to keep the included errors as low as possible, the methods for generating a load profile and wind power (WP) generation are chosen for each MV/HV transformer depending on the resulting mean absolute error (MAE) for the aggregated transformer power. For WP modeling it is chosen between the approaches WP and DM for each transformer specifically. In order to fit a transformer specific 24 h load profile different type of days and seasons are considered, more details can be found in [17].

For the wind farms, which are directly connected to the HV level, no further information is given except the installed capacity per node. Therefore, these units are represented by fitting a five parametric logistic function, described in equation 30 of [30], as a WTPC to the power curve of a wind turbine. The resulting WTPC is then scaled to the installed capacity of each wind farm. In order to calculate the generated

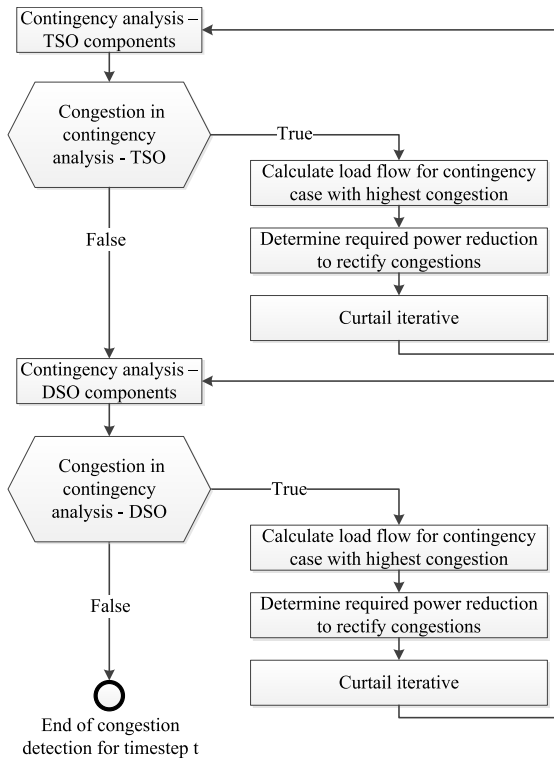


FIGURE 3. Process flow for congestion detection and curtailment prediction considering different voltage levels.

WP quarter hourly wind speeds are used, which are the nearest available wind forecast.

2) CONGESTION DETECTION

In order to detect congestions in the lines of the 110 kV distribution grid, or the transformers connecting the distribution with the transmission grid, a load flow calculation is realized in DIgSILENT PowerFactory. To guarantee the N-1 security, a contingency analysis is necessary. Furthermore dynamic line rating is installed for some lines and therefore also taken into account in the model.

In Germany transmission system operator (TSO) and distribution system operator (DSO) curtail REs as a preventive measure to maintain grid stability [19]. In reality, curtailment is requested when congestion is to be expected without considering any particular order between the system operators. In the model the congestion detection is first applied for components of the TSO and then performed for the DSO, taking curtailment requested by the TSO into account. The process flow is shown in Fig. 3.

First all contingency cases of the corresponding system operator are calculated, whereby in case of the TSO HV/EHV transformers and for the DSO the 110 kV lines are examined. In the event of a congested component the contingency case is selected which shows the highest component overloading. For the selected contingency case the load flow is calculated again and all the reductions of real power ΔP , that are required to rectify occurring congestions, are determined. ΔP_j denotes the difference between the current real power

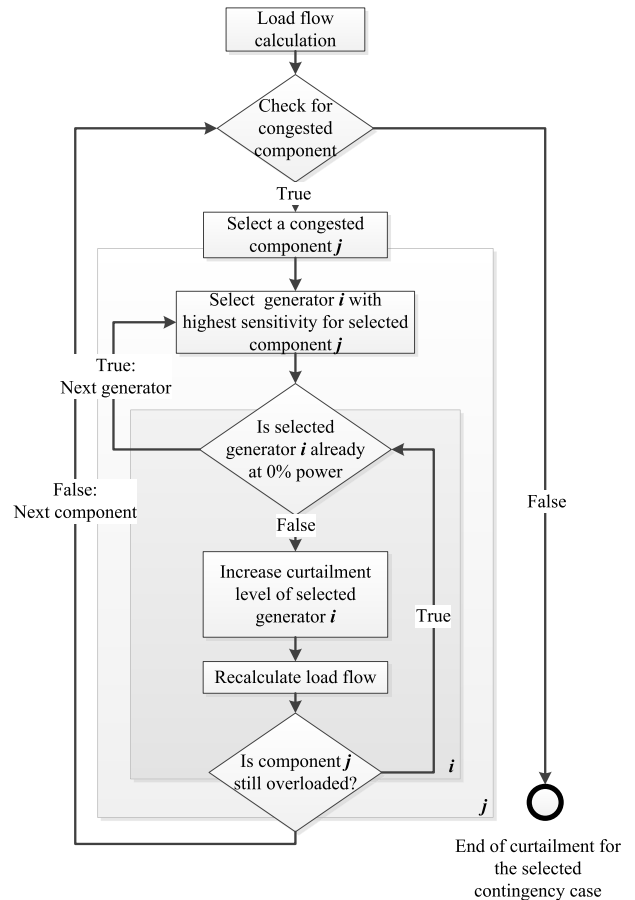


FIGURE 4. Process flow for curtailment considering a special contingency case.

P_j of a component j between two nodes I, L and its maximal permitted power P_j^{\max} [31], i.e.

$$\Delta P_j = P_j^{\max} - P_j. \quad (1)$$

P_j^{\max} is defined by (12) in [31]. Accordingly changes of voltage and reactive power are neglected and it can be described as

$$P_j^{\max} = \sqrt{3 \cdot (U_L \cdot I_{j,therm}^{\max})^2 - Q_j^2} \quad (2)$$

$I_{j,therm}^{\max}$ denotes the maximal current of the corresponding component. For some overhead lines in the distribution grid, dynamic line rating is implemented. In these cases $I_{j,therm}^{\max}$ is calculated according to [32]. The wind speed and temperature of coordinates close to the corresponding component are applied.

3) CURTAILMENT DETERMINATION ALGORITHM

ΔP_j is eliminated by defining curtailment in subject to an iterative increase of curtailment level and the numbers of curtailed wind farms. The first step is the calculation of the sensitivities for the nodes for all components. The corresponding sensitivity matrix, describing the impact of nodal changes, is determined by the linearization of the AC load flow equations around the current operational state and is thoroughly

described in [31]. Then each congestion is resolved following the iterative algorithm shown in Fig. 4.

The unit having the highest sensitivity on the corresponding component is chosen for curtailment starting with the lowest curtailment level: 60% of the nominal power. As long as the required power reduction ΔP_j is not fulfilled the level of curtailment is increased for the selected wind farm. If the highest level is reached and ΔP_j is still not zero, the next smaller sensitive unit is chosen to be curtailed.

C. QUANTIFYING UNCERTAINTY OF COMPONENT LOADING

Forecast are, by their nature, error-prone. In order to make them applicable for e.g. operating systems these errors should be considered [21]. In case of curtailment prediction the relevant variables are the loadings of the lines and transformers, which are determined by injections on n nodes and defined in the following as $\mathbf{P} = (\mathbf{P}_1, \dots, \mathbf{P}_n)$. As described by (14) in [25] the power flow on a component j can be determined by $P_j = \Lambda_j \mathbf{P}$, where Λ_j denotes the sensitivity values for the component j . Accordingly, the error of the active power flow on a component ϵ_j can be described by

$$\epsilon_j = \Lambda_j \tilde{\epsilon}, \quad (3)$$

where $\tilde{\epsilon} = (\tilde{\epsilon}_1 \dots, \tilde{\epsilon}_n)$ denote the errors of the node injections.

Therefore, the associated error can be interpreted as a multivariate RV and defined by the weighted sum of the errors of the node injections $\epsilon = \Lambda \tilde{\epsilon}$.

To estimate uncertainty of the component loadings, i.e. determining the corresponding distributions, several steps are carried out.

1) DETERMINATION OF THE NODE INJECTION ERROR DISTRIBUTION

As shown in Fig. 2 there are two kinds of nodes: MV/HV transformers and buses connecting greater wind farms with the HV level. For the MV/HV transformers measurement data exists and the errors of the predicted injection can be calculated.

In case of the wind power plants connected to transformers where no measurement of the power injections is available, the error has to be estimated in dependence of the predicted wind power. Therefore, a stochastic model is fitted to exemplary wind parks of the simulation region. The required measurement error ϵ was determined by calculating the generated wind power as described in section II-B1 and subtracting it from the corresponding measured power. For generalization the data is normalized to the installed capacity of the corresponding wind park. To estimate the error in dependence of the predicted WP, the data is assigned to certain intervals of the predicted WP. Distributions are selected using the Kolmogorov-Smirnov test [33] and fitted to the data of ϵ for each interval. In this way the error of predicted wind power can be sampled for each node, connecting the wind parks

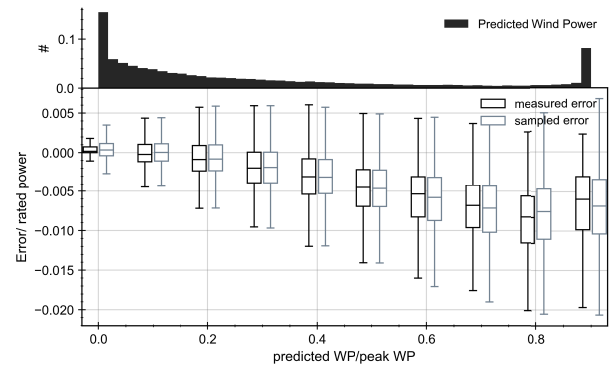


FIGURE 5. Correlation between the errors of the MV/HV transformers.

with the HV grid level considering the forecasted power, and denoted as i in

$$\epsilon_i | WP_i^{pred} \sim f_\epsilon(WP_i^{pred}) Peak_i \quad (4)$$

Finally the sampled error of a node has to be scaled with the corresponding peak power. For validation the error is sampled for exemplary wind parks. The resulting distributions are shown per bin as boxplots in Fig. (5). The distributions of the sampled error nearly fits these of the measured error. For predicted wind powers in the intervals $[0, .1)$, $[.8, .9)$ and $[.9, 1]$ the fitted error distributions have a wider spread. Since the occurrence of predicted power with normalized values around 0.0 or 0.9 is relatively high, a slight error in the sampled error should be considered. On the other hand less information exist for these wind farms which are simulated applying a manufacturer WTPC. So the error of the predicted wind power is estimated to be greater than that of the exemplary wind farms shown here. Therefore the deviations are acceptable.

2) DETERMINATION OF CUMULANTS

The distribution of a linear combination of various RV can be determined by applying cumulants in series expansion, like CFE [23], [25]. A cumulant κ of a RV is, like the corresponding central moment μ , a constant describing the RV's distribution and it can be expressed in relation to their central moments. The cumulants of the first orders $n \in \{1, 2, 3, 4\}$ are equal to the central moments with the same order: $\kappa_1 = \mu_1, \kappa_2 = \mu_2, \kappa_3 = \mu_3, \kappa_4 = \mu_4 - 3\mu_2^2$, whereas higher order cumulants can be calculated as in [34]:

$$\kappa_n = m_n - \sum_{k=1}^{n-1} \binom{n-1}{k-1} m_{n-k} \kappa_k \quad (5)$$

Having independent RVs, the multivariate cumulant of order \mathbf{n} is determined by its sum of marginal cumulants of order \mathbf{n} [35]. Considering the grid topology the cumulant with order \mathbf{n} of the multivariate RV ϵ_j is denoted as $\kappa_{\epsilon_j, \mathbf{n}}$ and can be calculated by applying the sensitivities $\Lambda_{j,1} \dots \Lambda_{j,m}$ of the RVs of the node errors and its corresponding cumulants $\kappa_{\epsilon_{1..n}}$:

$$\kappa_{\epsilon_j, \mathbf{n}} = \Lambda_{j,1}^{\mathbf{n}} \kappa_{\epsilon_{1, \mathbf{n}}} + \Lambda_{j,2}^{\mathbf{n}} \kappa_{\epsilon_{2, \mathbf{n}}} + \dots + \Lambda_{j,n}^{\mathbf{n}} \kappa_{\epsilon_{n, \mathbf{n}}} \quad (6)$$

3) CORNISH-FISHER EXPANSION

The Cornish-Fisher Expansion can be used to express the quantile function of a random variable Z as a power series in terms of the quantile function of the standard normal distribution. For this let Z^* denote the normalization of Z , i.e.

$$Z^* = \frac{Z - \mu_Z}{\sigma_Z}$$

We then have by [23]

$$Q_{Z^*}(q) \approx \xi(q) + \frac{\xi^2(q) - 1}{6} \kappa_3^* + \frac{\xi^3(q) - 3\xi(q)}{24} \kappa_4^* - \frac{2\xi^3(q) - 5\xi(q)}{36} (\kappa_3^*)^2 + \frac{\xi^4(q) - 6\xi^2(q) + 3}{120} \kappa_5^* - \frac{\xi^4(q) - 5\xi^2(q) + 2}{24} \kappa_3^* \kappa_4^* + \frac{12\xi^4(q) - 53\xi^2(q) + 17}{324} (\kappa_3^*)^3 \quad (7)$$

where Q_{Z^*} denotes the quantile function of Z^* , κ_j^* the j -th cumulant of Z^* , and ξ the quantile function of the standard normal distribution. Thus we have an approximation of Z^* and ξ the quantile function of the standard normal distribution.

4) IMPLEMENTATION OF UQ IN CURTAILMENT PREDICTION

To describe the uncertainty of component loading by corresponding cumulative distribution functions (CDFs), the errors of the node-injections have to be determined first. In the next step the line loading errors are determined by (3). Then two approaches determining the CDF of the loading errors are realized: CFE and determining the quantiles on basis of the empirical error distribution. The normalized distributions of the component loading errors are then expressed by cumulants. The line cumulants are used in the CFE to derive the quantiles of errors included in the line flow. Finally the received quantiles are transformed back into their distributions by $x = \sigma x^* + \mu$. As the CFE method can lead to errors in the tails [36], a rearrangement of the quantiles is realized according to [37] in the end. In the second approach the quantiles are taken by sorting the values of the empirical distribution and selecting these to the corresponding percentiles. In order to consider changes in the grid topology, the quantiles are calculated for each contingency.

D. USING UNCERTAINTY INFORMATION FOR CURTAILMENT PREDICTION

The uncertainty of the component loading is considered during the contingency analysis and curtailment. In Fig. 6 it is visualized how the errors of the predicted component loading and the probability of overloading are implemented.

In order to be adaptable to the behavior of the grid operator the forecast model has three parameters: the *threshold percentile*, the *lower threshold*, and the threshold for the *maximal component loading*. The *threshold percentile* defines

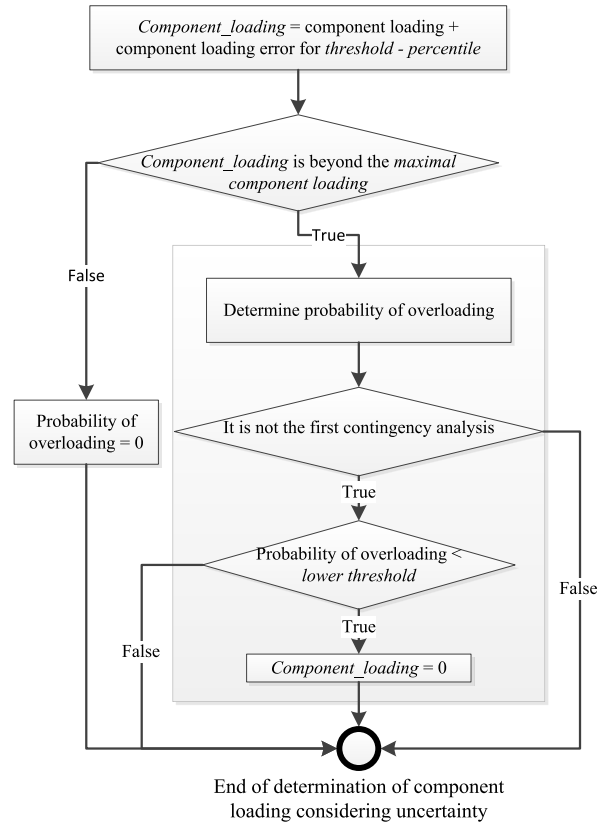


FIGURE 6. Determination of component loading considering errors and probability of overloading.

the maximal percentile that should be considered for the implemented error. The sum of the error percentile and the predicted component loading defines the loading which is finally considered during congestion detection (i.e. we consider $P_j^{\text{pred}} + q_\alpha(\epsilon_j)$, where P_j^{pred} denotes the predicted power flow on component j and $q_\alpha(\epsilon_j)$ the respective quantile of the error distribution for component j). So the higher the *threshold percentile* is, the greater becomes the component loading. Following an approach with a high security level, the *threshold percentile* applied in simulation is chosen to be 0.9. The *lower threshold* is applied if the contingency analysis (shown in Fig. 3) detects still congestions in the grid and leads to another iteration of curtailment. It defines a stop criterion by defining an acceptable probability for an overloading, which is chosen to be 30 % in this paper. The threshold for the *maximal component loading* defines congestions and for this paper a values of 100 % is taken. These thresholds are individually adaptable and allow to tune the curtailment prediction according the required security level.

So the process of determining congestions with considering uncertainties can be described by following steps: First it is checked whether a component is congested considering the *threshold percentile* of the error. Is the component overloaded (i.e. $P_j^{\text{pred}} + q_\alpha(\epsilon_j) > P_j^{\text{max}}$) the probability of its overloading is determined: starting with the lowest error-percentile and increasing the percentile as long as a congestion occurs or the

threshold percentile is reached. Then it is checked, whether it is the first contingency analysis. If this is not the case, the congestion probability is compared against the *lower threshold*. In case of a probability smaller than the *lower threshold*, the component is not considered congested in the following. The same happens if no congestion is detected for the component.

In the process of iterative curtailment the uncertainty of the component loading is considered by processing the overloaded components in a descending order of the required power reduction weighted by the probability of overload. If the iteration for the time step and voltage level is not the first, only these congested components are considered, which have a probability higher than the *lower threshold*. Then the first congested component is selected and the generator with the highest sensitivity for the selected component is chosen for curtailment. As long as the congestion remains and the generator is not at 0% power, the curtailment level is increased, starting with curtailment level of 60%, the load flow is calculated again and the congested components including the errors and the probabilities are determined and sorted again for the new grid situation. If the selected generator is at 0% power a new generator is selected on basis of its sensitivity. The process is repeated so long until no component with a weighted congestion greater zero is left.

III. MODEL VALIDATION

A. DESCRIPTION OF DATA AND GRID

The proposed method is applied to a realistic 110 kV distribution grid provided by the corresponding grid operator with a high share of installed wind power. A scheme of the grid is shown in Fig. 7. The HV topology is mainly characterized by its double ring structure of its lines (described by 5). There are several nodes, which can be separated into three groups: one type has connected consumers and generation (described by 2) and one has only consumers connected (described by 4). Both are simulated according MV/HV transformer model described in our previous work [17]. 3 represents nodes connecting wind farms with the HV grid. There are 61 nodes in total, of which are 6 nodes of 4, 40 nodes of 2, and 15 are nodes of 3. Only the HV/EHV transformers (described by 1) and the 220 kV lines (described by 7) connecting the HV/EHV transformers and the external grid (described by 6), represented by a reference node, are the components of the TSO which are simulated. Congestions are considered for the HV/EHV transformers and the lines of the 110 kV grid.

The simulation was done for February, 2016 with a time step of 15 minutes. The meteorological data was available for the coordinates of the MV/HV transformers. The wind speed was provided hourly by DWD (Deutscher Wetterdienst) [38] for a height of 73 m. To adapt it to the simulation time step, the wind speed was interpolated and the resulting error is assumed to be acceptable [17]. The global irradiation is based on Meteosat-SEVIRI data [39] with a temporal

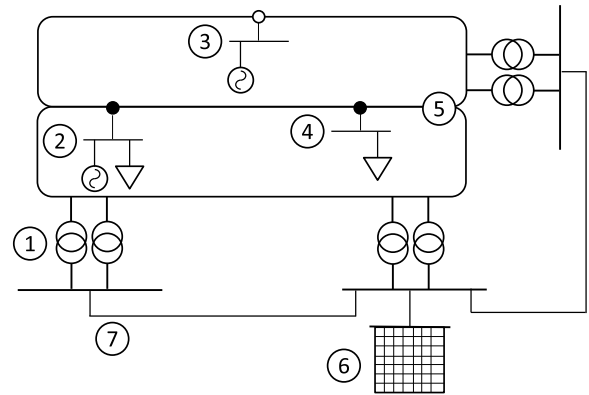


FIGURE 7. Schematic of the simulated distribution grid.

resolution of 15 minutes. For the MV/HV model the corresponding DSO provided measurements of the power flow for 2 years with a temporal resolution of 15 minutes. Also the installed capacities of each power plant type are known for the transformers.

In order to analyze the influence of the period of available data for model adjustment for the MV/HV transformers (see chapter II-B1) and to validate the curtailment approach, different scenarios are considered. The *benchmark* scenario is applied to proof the validity of the implemented curtailment approach. For this scenario measured data of a time period of 2 years is used to fit the load profiles and WP functions and the same time period is simulated in a second step. Whereas the scenarios *1yr* and *6m* use a certain time slot of the measured data to adjust the MV/HV transformer model. In case of the *1yr* scenario, the measured data of the first year is used for model fitting and the second year is simulated. For the *6m* scenario it works analog with six months.

The calculations were deployed on 64-bit windows machine with an Intel®Core i5-6500 CPU @ 3.20GHz and 16 GB RAM. The programming language was python and the power flow simulations were calculated with DIGSILENT PowerFactory.

B. COMPONENT LOADING ERROR

Two approaches of determining the quantiles of the loading errors are applied in the prediction of curtailment: CFE and the determination of quantiles on basis of the empirical distribution. The resulting CDFs determined for one contingency case are visualized for two components in Fig. 8. The error is visualized as the error of the real power in percentage of the maximal permitted real power. As the CFE quantiles are approximated by using only 5 values, these show larger deviations than the empirical quantiles. Comparing the CFE-quantiles of both components it becomes apparent, that the component of the upper plot shows a similar smooth course like the empirical CDF, whereas those of the lower plot has a continuous but not differentiable function. This behavior results from the rearrangement, due to incorrect tails in the approximated CDF.

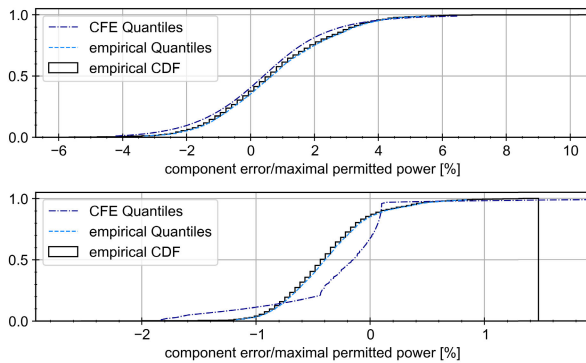


FIGURE 8. CDFs describing the component loading error for different objects, determined empirically and by CFE.

C. VALIDATION OF THE GRID MODEL AND THE CURTAILMENT APPROACH

The grid model and the curtailment approach is validated by comparing to historic curtailment. For this purpose the time series calculated according to the benchmark scenario are used for the simulation of one month. The occurrence of all determined curtailment is compared to the times of the historical curtailment using the so called Sørensen Dice coefficient, which was separately developed by Sørensen [40] and Dice [41]. The Sørensen Dice coefficient is a measure for similarity and if applied for booleans it can be expressed as shown in (8), whereas the true negatives are excluded. In the formula TP denotes the true positive values, FP the false positives, and FN the false negatives values.

$$S_{Dice} = \frac{2TP}{2TP + FP + FN} \quad (8)$$

The Sørensen Dice coefficient and its parameters TP , FP , and NP determined for the *benchmark* scenario are shown in Table 1. According to the coefficient for the aggregated curtailment of both voltage levels, a high similarity between historic and simulated curtailment is reached. This indicates that a big amount of congestions are correctly timed. When considering the voltage levels separately, the Sørensen Dice coefficient shows a better match for congested components of the TSO than for congested DSO components. Furthermore, congestions are overestimated in the DSO grid, which is shown by the parameter FP , that is significant higher than for the aggregated case or TSO. But the accuracy of the temporal match of curtailment is aggregated higher than for the single voltage levels. This suggests that the error results from the differentiation between the grid levels. The difference between FP and FN is the lowest for TSO and it also shows the highest number of not detected congestion indicates, that these missed congestions on the HV/EHV transformers leads to more congestions in the distribution grid. Taking the high amount of matches in the aggregated case and a detection rate of 95% for true negatives, it can be deduced that the curtailment algorithm has a adequate efficiency for predicting the right times of congestions.

TABLE 1. Sørensen dice coefficient, TP, FP, FN shown for *benchmark* scenario in percentage of the number of calculated times in the simulation period.

grid	Sørensen Dice coefficient	TP (percentage)	FP (percentage)	FN (percentage)
Aggregated	0.85	0.21	0.06	0.01
TSO	0.80	0.15	0.04	0.03
DSO	0.48	0.09	0.18	0.006

TABLE 2. Sørensen dice coefficients for simulated curtailment visualized for the different scenarios.

grid	Benchmark	1 yr	6m	6m - CFE quantiles	6m - empirical quantiles
Aggregated	0.85	0.80	0.84	0.83	0.84
TSO	0.80	0.78	0.79	0.79	0.81
DSO	0.48	0.44	0.47	0.46	0.47

In Table 2 the calculated Sørensen Dice coefficients for the time series scenarios are shown. The *6m* scenario, additional uncertainties have been considered. As a consequence the scenario is calculated two more cases: one time considering the CFE quantiles and the other considering empirical quantiles. The results show, that the scenarios differentiate in their accuracy. Starting with the coefficients for the aggregated curtailment, the scenario *6m* has nearly as much matches as the benchmark scenario, whereas the accuracy of *1yr* is a little lower. This indicates that the modeled load profiles and power curves of the scenario *6m* fit the historic time series better than that of *1yr*. This can be confirmed by the MAE determined for the calculated transformer power, excluding times of curtailment, for both scenarios: The MAE for *6m* is 3.61 MW and so smaller than that for *1yr*, which makes 3.90 MW. One possible explanation could be that the spread in the data, which is used for fitting, is smaller in the *6m* than in the *1yr* scenario. As in the *benchmark* case, both scenarios show a higher accuracy for congested TSO components than for components of the DSO.

For the *6m* scenario the consideration of uncertainty is implemented according to section II-C4. As Fig. 8 suggested the simulation using CFE based quantiles shows lower values for the Sørensen Dice coefficients than those of the simulation using the empirical quantiles. The lower accuracy for CFE quantiles compared to the *6m* scenario without considering uncertainty, at DSO grid level, can be caused by the deviations included in the quantiles. Having in case of the empirical quantiles better values than for the *6m* scenario without uncertainty considered, indicates that these quantiles are a good representation of the real errors for the component loading. Furthermore, it can be assumed that the quantiles for TSO components are more accurate than those for DSO components, as the coefficients are equal or even better for TSO taken the uncertainty into account, whereas the coefficients for DSO are worse or equal. One explanation could be that the HV/EHV transformers are not that sensitive to e.g. topology changes as the 110 kV lines are.

TABLE 3. f1-score shown for the 6m scenario and the short term congestion prediction of transmission grids proposed in [2].

prediction approach	precision	recall	f1-score
6m scenario	0.77	0.92	0.84
[2]	0.70	0.64	0.65

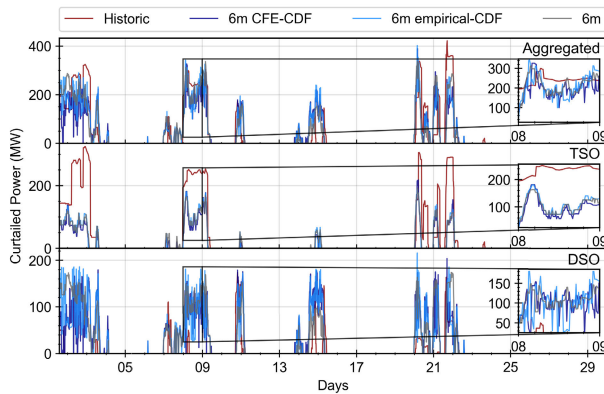


FIGURE 9. Curtailed power over time separated per power level and visualized for the 6m simulation scenario considering CFE- and empirical quantiles.

For further validation of the approach the f1-score [42] is calculated for the 6m scenario. In Table 3 the results are compared to the f1-score of the congestion forecast model for transmission grid proposed in [2]. It can be seen that the proposed method of this paper has a sufficient accuracy for the timing of congestion prediction. But it has to be considered that in [2] the German transmission grid is simulated, whereas in the proposed approach the HV level of the distribution grid and the connected HV/EHV-transformers are modelled. Furthermore, the 6m scenario is simulated with a 15 minute time step, whereas the time step in [2] is hourly.

Fig. 9 shows the resulting curtailed power simulated with the 6m scenario and also considering the CFE quantiles and the empirical quantiles in load flow calculations. Concerning the frequency of the aggregated curtailed power the simulated one often shows peaks at the same time where the historic one does. But as can be seen in the zoomed area, in contrast to the historic curtailed power, the simulated one happens to have more fluctuations. This could be caused by the fact that in the model the required curtailment is determined for each time step separately, in contrast to realistic grid operations in contrast to realistic grid operation where the operations of feed in management needs to be as less as possible. As a consequence of adjusting curtailment to the requirements of each time step, the simulated curtailed power is less than those of the historic ones. Comparing between the voltage levels shows greater deviations in amplitude. Whereas the amount of simulated curtailed power is underestimated for TSO it is overestimated for DSO. This indicates that the transmission capacity of the TSO-transformer tends to be overestimated. As the TSO curtails less, more power is available in the distribution grid and as a consequence more congestions are

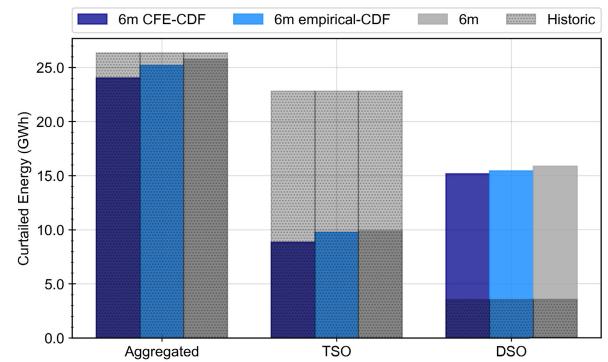


FIGURE 10. Curtailed energy for a simulation time period of one month, separated per power level and visualized for the 6m simulation scenario considering CFE- and empirical quantiles.

TABLE 4. Pearson correlation for component loading and input parameters.

	wind speed	global irradiance	hour of the day	temperature
mean of absolute values	0.5	0.11	0.2	0.43
maximum	0.87	0.24	0.76	0.86
minimum	-0.43	-0.4	-0.40	-0.71

calculated for the 110 kV lines. Since most of the DSO curtailment appears at times of historic TSO curtailment, the matches between historic and simulated DSO curtailment are poor, as the Sørensen Dice coefficients also indicated.

In Fig. 10 the simulated curtailed energy of the 6m scenario, considering in two cases uncertainty and in one none, is compared to the historic one, differentiated between the aggregated amount and the two voltage levels. As a possible outcome of the step wise determination of curtailment, the aggregated simulated curtailed energy for the three scenarios is between 0.59 GWh and 2.31 GWh smaller than the historic one. This makes a small deviation between 2.23 % and 8.78 % of the historical aggregated curtailed energy. A high underestimation of curtailed energy around 13 GWh is determined for TSO, which causes a high overestimation of curtailed energy of around 11 GWh for DSO. The consideration of loading errors leads for both voltage levels to lower amounts of curtailed energy than without. Furthermore, the empirical quantiles seem to consider smaller errors than the CFE based quantiles, which is indicated by the lower curtailed energy for CFE- than for empirical-CDFs.

D. INFLUENCE OF INPUT PARAMETERS

In the following the input parameter with the highest impact on the results is analyzed. Table 4 shows the minimum, maximum, and mean of the pearson correlations between component loading and the parameters wind speed, global irradiance, hour of the day and temperature. According to the correlation coefficients wind speed has the highest impact on component loading, wherefore the following analysis will focus on this parameter.

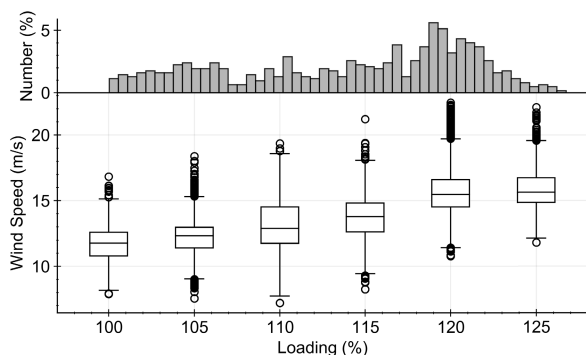


FIGURE 11. Distribution of wind speed per loading of a component. The histogram in the upper figure describes the frequency of component loading.

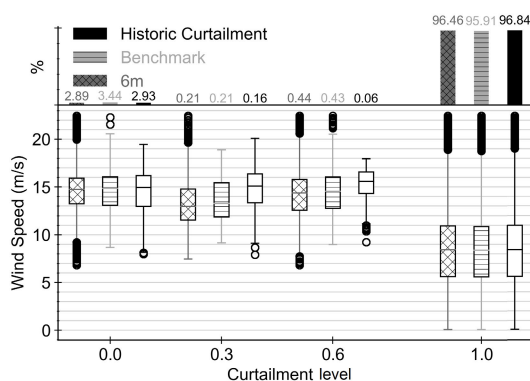


FIGURE 12. Frequency per curtailment level and the corresponding wind speed distributions occurring in the model region at the corresponding times.

The correlation between loading of one 110 kV line and wind speed becomes apparent in Fig. 11, considering only data at times of congestion. The figure shows an increase of wind speed with increasing loading. So in this area with a high installed capacity of WP, the parameter wind speed has a great impact on the accuracy of the curtailment predictions. The loading of a line is influenced by its neighborhood to connected loads, REs, and simulated contingencies. The lowest wind speed at times of simulated congestions for all components is 7.20 m/s.

In Fig. 12 the distribution of wind speeds occurring in the model region at the corresponding times is shown for each curtailment level in boxplots. Also the number of curtailments are visualized per level. The levels are shown from 1.0 to 0.0, where 1.0 represents times of no curtailment and 0.0 means an infeed reduction to 0.0.

The bars at the top visualize the percentage of the data set (simulation period for each RE unit) per curtailment level. It is shown that the number of curtailments decreases from benchmark scenario to the historic curtailment to 6m scenario. Overall the number of the simulated curtailments is for each scenario higher than that of the historic ones. This indicates that more congestions are simulated than actually happened. As in the case of historic curtailment the number of curtailment decreases from level 0.0 to 0.3, but instead

of having hardly any curtailment of level 0.6, the simulated curtailments shows a higher number than for level 0.3.

In the following, the impact of wind speed on the curtailment level is analyzed. At times of no curtailment the distribution of wind speed corresponds, whereas the wind speeds tend to be lower for simulation compared to historic curtailment at level 0.3 and 0.6. The lower wind speeds suggest, that congestions are reached earlier than it was in history. This shift in the distribution of wind speed could be caused by lower consumption, whereby more power remains in the grid. Accordingly the wind speed distribution of the 6m scenario is lower, where the modeled load profiles are used, than that of the benchmark scenario, where the measured power of each node subtracted from the generated wind power was applied.

IV. DISCUSSION

Proposing a forecast model for short-term curtailment prediction contributes to an efficient management of curtailment, that has been increasingly occurred due to the mismatch between the growth of RE integration and grid expansion. Furthermore, the transition of feed-in management into redispatch at the end of 2021 in Germany, makes such a short-term curtailment prediction for distribution grids more urgent. Reaching a good match of predicted congestions and showing only little deviations of predicted curtailed energy, makes this model to a valuable tool for system operators in their operational business.

As the proposed approach is in an early stage of development, analysis regarding computational cost was not considered during this work. In order to give an overview of the potential computational costs anyway, a rough analysis was performed measuring the computation time for one time step in simulation. The results show variations between 22 seconds and 2.9 minutes, depending if a congestion was detected, which has a higher computational effort, or not. Improving the computational costs should be the topic of further development.

The results indicate that a time period for maintenance of every 6 month for the MV/HV-model gets the highest precision. The historic data of the past six month are applied for power curves and load profiles fitting in order to keep the model updated and adjust it to occurring changes in installed RE capacity or consumption patterns. In case of congestions, caused by the DSO, greater errors in the match of congestions as well in the amount of curtailed energy appear. These deviations of curtailment prediction are the consequence of not determined overloadings on TSO components. Determining less congestions on TSO transformers can be brought about by assuming a high transmission capacity of the transformers or a selection of the wrong contingencies, which lead to a different power flow in the topology resulting in less power arriving at the transformers.

However, it has to be considered, that the system operator tend to have as less operations as possible, which has not been considered in the proposed model. Furthermore the objective to reduce any possibility for an event of a contingency, could

also lead to a higher amount of curtailed energy. Consequential deviations between simulated and historic curtailment occur.

One input-parameter, which has a great influence on the prediction accuracy is wind speed. Having a high installed capacity of wind energy in the model region, WP is the most represented RE type and therefore has the greatest impact and, as the results indicate, also a direct effect on component loading. Schermeyer *et al.* proofed via sensitivity analysis that the simulated WP has even a higher influence on the uncertainty than the grid parameters [16]. So in order to increase accuracy of curtailment prediction wind speed forecasts with a high precision should be applied. Furthermore, wind speed data plays also an important role at the identification of historical WP or consumption in the measured vertical power of MV/HV transformers applied in adjustment of the MV/HV models as described in our previous work [17]. So having wind speed data with a higher precision, leads to an increased accuracy of identified consumption and WP, and therefore to better conditions for load profile and power curve fitting. It has to be considered that in regions, where a different kind of RE type is prevailing, it's corresponding input parameter has the major impact on the component loading.

As a reliable interpretation of predictions require information about their uncertainty, the determination of congestions, and the resulting decision to curtail for two scenarios of the proposed model is based on loading errors and the consequential probabilities. The analyzed scenarios follow a conservative strategy by determining the required power reduction for an error of a 0.9 percentile and a congestion probability with minimum 30%. Consequently working with lower probabilities to determine component loading and the threshold determining the necessity to curtail, would lead to a smaller amount of curtailed power. That the scenarios with uncertainty quantification curtail less than those without, shows that the component loading tends to be overestimated without considering their probabilities. Integrating the proposed prediction model in feed in management could therefore reduce the spillage of energy caused by curtailment. That the deviation of curtailed energy between the uncertainty quantification based scenarios and historic curtailment is bigger than those for the scenario without considering uncertainty is caused by two things: On the one hand, the CDFs describing the errors are adjusted on basis of a selection of data for a certain period, which leads to kind of an average error and neglects the influence of different input parameters. Therefore an input parameter dependent description of the error CDF should be analyzed in future work. On the other hand the consideration of different contingencies brings a certain risk. Having variations between the CDFs of different contingencies for one component, an incorrect contingency means therefore, besides an imprecise load flow and consequently erroneous congestions, that the wrong errors are taken into account. The error quantiles are determined with two different approaches and it is shown that the empirical CDFs are more accurate than those based on CFE. A good

reason to choose CFE for quantile determination anyway, is that it only requires five values, the cumulants, to fit the CDF, instead of the whole data set. So if system operators try to model the grid of another system operator, which is connected to their own, the only data that needs to be exchanged to consider the uncertainty are the cumulants. Whereas empirical quantiles seem to be the better choice, if the data is accessible anyway.

The validity of the proposed approach was proven for a real distribution grid. Nevertheless, this model can be transferred to any HV distribution grid, if following data is available: the corresponding grid topology, historic measurement of the vertical power flow on the connected MV/HV transformer for a time period of at least six months and the installed capacity of each RE type per node. Furthermore, to model the vertical power flow on MV/HV transformers, the lower grid levels should be supplied by one transformer at the time. In order to determine congestions in the HV grid level all nodes (MV/HV and HV/EHV) should be modeled to get all in-coming and out-flowing power flows. A transfer of this approach to EHV grid level should be possible, if the mentioned requirements are fulfilled. But it has to be considered, that only those congested components are detected, which are represented in the simulated grid. However, other grids or voltage levels have not been tested within this study.

V. CONCLUSION

RE curtailment due to grid congestions means a spillage of renewable energy and it requires optimization. Furthermore, the regulation of RE curtailment occurred in distribution grids will be transitioned into redispatch in Germany, which involves congestion prediction. Proposing a novel approach of a short-term curtailment prediction in distribution grids considering uncertainties meets the requirement for future grid operation in Germany. Additionally, it allows, providing the knowledge of potential amount and location of curtailed energy, to optimize the deployment of flexibility options. The integrated possibilities of congestions can help to interpret the given prediction. To gain a better accuracy in the prediction of voltage level specific forecasts, some adjustments are still required. However, the model shows predictions with auspicious accuracy, therefore it can help the grid operator to gain valuable insights into his grid.

ACKNOWLEDGMENT

The authors thank Deutscher Wetterdienst for wind speed analysis data of the COSMO-DE model and all project partner of the research project "enera", which is funded by the Federal Ministry for Economic Affairs and Energy (BMWi, grant no. 03SIN317). They also thank EWE NETZ GmbH for providing time series of aggregated load and Avacon Netz GmbH for the provision of their grid model.

REFERENCES

- [1] H. K. Jacobsen and S. T. Schröder, "Curtailment of renewable generation: Economic optimality and incentives," *Energy Policy*, vol. 49, pp. 663–675, Oct. 2012.

- [2] P. Staudt, B. Rausch, J. Gärtner, and C. Weinhardt, "Predicting transmission line congestion in energy systems with a high share of renewables," in *Proc. IEEE Milan PowerTech*, Jun. 2019, pp. 1–6.
- [3] P. Denholm, "Energy storage to reduce renewable energy curtailment," in *Proc. IEEE Power Energy Soc. Gen. Meeting*, Jul. 2012, pp. 1–4.
- [4] *Leitfaden zum EEG-Einspeisemanagement—Abschaltrangsfolge, Berechnung von Entschädigungszahlungen und Auswirkungen auf die Netzentgelte*, Bundesnetzagentur für Elektrizität, Gas, Telekommunikation, Post und Eisenbahnen, Bonn, Germany, 2014.
- [5] *Gesetz zur Beschleunigung des Energieleitungsbaus*, Bundesgesetzblatt Jahrgang Teil I, Nr. 19, Bonn, Germany, May 2019.
- [6] *Redispatch als teil des marktlichen engpassmanagements*, BDEW Bundesverband der Energie- und Wasserwirtschaft. E. V., Berlin, Germany, Aug. 2015.
- [7] D. Liu, H. Cheng, J. Lv, Y. Fu, and J. Zhang, "Probability constrained optimisation model for transmission expansion planning considering the curtailment of wind power," *J. Eng.*, vol. 2019, no. 18, pp. 5340–5344, Jul. 2019.
- [8] T. Bongers, J. Kellermann, M. Franz, and A. Moser, "Impact of curtailment of renewable energy sources on high voltage network expansion planning," in *Proc. Power Syst. Comput. Conf. (PSCC)*, Jun. 2016, pp. 1–8.
- [9] P. Wiest, K. Frey, K. Rudion, and A. Probst, "Dynamic curtailment method for renewable energy sources in distribution grid planning," in *Proc. IEEE Power Energy Soc. Gen. Meeting (PESGM)*, Jul. 2016, pp. 1–5.
- [10] L. Michi, M. Migliori, A. C. Bugliari, B. Aluisio, G. M. Giannuzzi, and E. M. Carlini, "Transmission network expansion planning: Towards enhanced renewable integration," in *Proc. AEIT Int. Annu. Conf.*, Oct. 2018, pp. 1–5.
- [11] A. Kulmala, S. Repo, and J. Pylvänäinen, "Generation curtailment as a means to increase the wind power hosting capacity of a real regional distribution network," *CIREN-Open Access Proc. J.*, vol. 2017, no. 1, pp. 1782–1786, Oct. 2017.
- [12] A. N. M. M. Haque, D. S. Shafiullah, P. H. Nguyen, and F. W. Blik, "Real-time congestion management in active distribution network based on dynamic thermal overloading cost," in *Proc. Power Syst. Comput. Conf. (PSCC)*, Jun. 2016, pp. 1–7.
- [13] A. N. M. M. Haque, P. H. Nguyen, T. H. Vo, and F. W. Blik, "Agent-based unified approach for thermal and voltage constraint management in LV distribution network," *Electr. Power Syst. Res.*, vol. 143, pp. 462–473, Feb. 2017.
- [14] Q. Zhou, L. Tesfatsion, and C.-C. Liu, "Short-term congestion forecasting in wholesale power markets," *IEEE Trans. Power Syst.*, vol. 26, no. 4, pp. 2185–2196, Nov. 2011.
- [15] D. Peters, W. Heitkoetter, R. Völker, A. Möller, T. Gross, B. Petters, F. Schuldt, and K. V. Maydell, "Validation of an open source high voltage grid model for AC load flow calculations in a delimited region," *IET Gener., Transmiss. Distrib.*, vol. 14, no. 24, pp. 5870–5876, Dec. 2020.
- [16] H. Schermeyer, C. Vergara, and W. Fichtner, "Renewable energy curtailment: A case study on today's and tomorrow's congestion management," *Energy Policy*, vol. 112, pp. 427–436, Jan. 2018.
- [17] E. Memmel, D. Peters, R. Völker, F. Schuldt, K. Maydell, and C. Agert, "Simulation of vertical power flow at MV/HV transformers for quantification of curtailed renewable power," *IET Renew. Power Gener.*, vol. 13, no. 16, pp. 3071–3079, Dec. 2019.
- [18] Y. Gu and L. Xie, "Fast sensitivity analysis approach to assessing congestion induced wind curtailment," *IEEE Trans. Power Syst.*, vol. 29, no. 1, pp. 101–110, Jan. 2014.
- [19] *VDE-AR-N 4140 Kaskadierung von Maßnahmen für Die Sicherheit von Elektrischen Energieversorgungsnetzen*, VDE Verlag GmbH, Berlin, Germany, Feb. 2017.
- [20] T. Gross, S. Reese, B. Petters, M. Cupelli, D. Mildt, and A. Monti, "A novel approach to DG curtailment in rural distribution networks—A case study of the Avacon grid as part of the InterFlex field trial," in *Proc. IEEE 16th Int. Conf. Ind. Informat. (INDIN)*, Jul. 2018, pp. 667–672.
- [21] J. Miettinen, H. Holtinen, J. Ämmälä, and M. Piironen, "Wind power forecasting at transmission system operator's control room," in *Proc. IEEE Power Energy Soc. Gen. Meeting*, Jul. 2015, pp. 1–5.
- [22] Y. Li, Z. Yang, G. Li, D. Zhao, and W. Tian, "Optimal scheduling of an isolated microgrid with battery storage considering load and renewable generation uncertainties," *IEEE Trans. Ind. Electron.*, vol. 66, no. 2, pp. 1565–1575, Feb. 2019.
- [23] M. Aien, A. Hajebrahimi, and M. Fotuhi-Firuzabad, "A comprehensive review on uncertainty modeling techniques in power system studies," *Renew. Sustain. Energy Rev.*, vol. 57, pp. 1077–1089, 2016. [Online]. Available: <https://www.sciencedirect.com/science/article/pii/S1364032115014537>, doi: 10.1016/j.rser.2015.12.070.
- [24] F. J. Ruiz-Rodríguez, J. C. Hernández, and F. Jurado, "Probabilistic load flow for photovoltaic distributed generation using the Cornish–Fisher expansion," *Electr. Power Syst. Res.*, vol. 89, pp. 129–138, Aug. 2012.
- [25] J. Usaola, "Probabilistic load flow in systems with wind generation," *IET Gener., Transmiss. Distrib.*, vol. 3, pp. 1031–1041, Dec. 2009.
- [26] M. Fan, V. Vittal, G. T. Heydt, and R. Ayyanar, "Probabilistic power flow studies for transmission systems with photovoltaic generation using cumulants," *IEEE Trans. Power Syst.*, vol. 27, no. 4, pp. 2251–2261, Nov. 2012.
- [27] E. Ciapessoni, D. Cirio, A. Pitto, S. Massucco, and F. Silvestro, "A novel approach to account for uncertainty and correlations in probabilistic power flow," in *Proc. IEEE PES Innov. Smart Grid Technol., Eur.*, Oct. 2014, pp. 1–6.
- [28] M. Marrocu and L. Massidda, "A simple and effective approach for the prediction of turbine power production from wind speed forecast," *Energies*, vol. 10, no. 12, p. 1967, Nov. 2017.
- [29] M. Lydia, A. I. Selvakumar, S. S. Kumar, and G. E. P. Kumar, "Advanced algorithms for wind turbine power curve modeling," *IEEE Trans. Sustain. Energy*, vol. 4, no. 3, pp. 827–835, Jul. 2013.
- [30] M. Lydia, S. S. Kumar, A. I. Selvakumar, and G. E. P. Kumar, "A comprehensive review on wind turbine power curve modeling techniques," *Renew. Sustain. Energy Rev.*, vol. 30, pp. 452–460, Feb. 2014.
- [31] I. Liere-Netheler, F. Schuldt, K. Maydell, and C. Agert, "Optimised curtailment of distributed generators for the provision of congestion management services considering discrete controllability," *IET Gener., Transmiss. Distrib.*, vol. 14, no. 5, pp. 735–744, Mar. 2020.
- [32] B. Muratori, *IEEE Standard for Calculating the Current-Temperature Relationship of Bare Overhead Conductors*, IEEE Standard, 2013, pp. 738–2012.
- [33] W. Feller, *On the Kolmogorov–Smirnov Limit Theorems for Empirical Distributions*. Cham, Switzerland: Springer, 2015, pp. 735–749.
- [34] A. DasGupta, *Fundamentals of Probability: A First Course*. New York, NY, USA: Springer, 2010.
- [35] P. McCullagh, *Tensor Methods in Statistics: Monographs on Statistics and Applied Probability*. London, U.K.: Chapman & Hall, 2018.
- [36] D. L. Wallace, "Asymptotic approximations to distributions," *Ann. Math. Statist.*, vol. 29, no. 3, pp. 635–654, Sep. 1958.
- [37] V. Chernozhukov, I. Fernández-Val, and A. Galichon, "Rearranging Edgeworth–Cornish–Fisher expansions," *Econ. Theory*, vol. 42, no. 2, pp. 419–435, 2010.
- [38] M. Baldauf, J. Förstner, S. Klink, T. Reinhardt, C. Schraff, A. Seifert, and K. Stephan, *Kurze Beschreibung des Lokal-Modells Kurzfrist COSMO-DE (LMK) und seiner Datenbanken auf dem Datenserver des DWD*. Offenbach, Germany: Deutscher Wetterdienst, 2016.
- [39] A. Hammer, J. Kühnert, K. Weinreich, and E. Lorenz, "Short-term forecasting of surface solar irradiance based on Meteosat-SEVIRI data using a nighttime cloud index," *Remote Sens.*, vol. 7, no. 7, pp. 9070–9090, Jul. 2015.
- [40] T. Sørensen, "A method of establishing groups of equal amplitude in plant sociology based on similarity of species content and its application to analyses of the vegetation on danish commons," *Biol. Skr.*, vol. 5, no. 4, 1948.
- [41] L. R. Dice, "Measures of the amount of ecologic association between species," *Ecology*, vol. 26, no. 3, pp. 297–302, Jul. 1945, doi: 10.2307/1932409.
- [42] D. M. Powers, "Evaluation: From precision, recall and F-measure to ROC, informedness, markedness and correlation," *J. Mach. Learn. Technol.*, vol. 2, no. 1, pp. 37–63, 2011.



ELENA MEMMEL received the B.Sc. degree in geocology from the Technical University of Freiberg, Germany, in 2014, and the M.Sc. degree in environmental modeling from the University of Oldenburg, Germany, in 2017. She is currently pursuing the Ph.D. degree with the Department of Energy Systems Technology, DLR Institute of Networked Energy Systems, Oldenburg, Germany. Her research interests include but are not limited to renewable energy integration, modeling and simulation of power system operation and uncertainty quantification.



SUNKE SCHLÜTTERS received the Ph.D. degree in pure mathematics from Carl von Ossietzky University of Oldenburg, Germany, in 2015. In 2018, he switched to the field of energy management research. He is currently working as a Researcher and a Project Manager working on energy management strategies and algorithms with the DLR Institute of Networked Energy Systems. His research interest includes machine learning based self-optimizing energy management systems.



RASMUS VÖLKER received the master's degree in electrical engineering with the specialization in electrical energy technology from the Kiel University of Applied Science, Germany, in 2015. Since 2015, he has been working as a Project Manager with the Department of Energy Systems Technology, DLR Institute of Networked Energy Systems, Oldenburg, Germany. His main research interests include reliable power grids with a high share of flexible and decentralized generation.



FRANK SCHULDT received the Diploma degree in electrical engineering from the University of Applied Science Emden, Germany, in 1994. From 1994 to 2011, he held various industrial positions. He is currently the Deputy Head of the Department of Energy Systems Technology and the Head of the Flexibility Options and Grid Services Group, DLR Institute of Networked Energy Systems, Oldenburg, Germany. His research interests include the integration of flexibility options in energy systems, reliability, availability, maintainability and safety in power grids, and the design of system services for energy systems with high share of power electronic based generation.



KARSTEN VON MAYDELL received the B.A. and M.Sc. degrees in physics from the University of Oldenburg, Germany, in 1997 and 2000, respectively, and the Ph.D. degree in physics from the University of Marburg, Germany, in 2003. From 2000 to 2006, he worked as a Graduate Research Assistant and a Postdoctoral Researcher and a Project Manager with the Helmholtz-Zentrum Berlin. From 2006 to 2007, he worked as a Project Manager Research and Development at Q-Cells AG in Thalheim, Germany. From 2007 to 2008, he was a Group Leader of the Energy and Semiconductor Research Laboratory, University of Oldenburg. He was the Head of the Division of Photovoltaics, from 2008 to 2014, and the Head of the division Energy Systems and Storage, from 2014 to 2017, at the NEXT ENERGY Research Institute, Oldenburg, Germany. Since 2017, he has been the Head of the Department of Energy Systems Technologies, DLR Institute of Networked Energy Systems. His research interests include the design of energy systems, smart energy management for grid connected and off-grid energy systems, integration of flexibilities in energy systems, robust operation of power grids, and power electronics design.



CARSTEN AGERT studied Physics at the University of Marburg, Germany, and the University of Canterbury, U.K. As a scholar of the Studienstiftung, he completed his Ph.D. in Physics in 2001, based on his research work at the Fraunhofer Institute for Solar Energy Systems in Freiburg, Germany, and at the University of Oxford, U.K. In 2001, he worked as a Postdoctoral Researcher in Pretoria, South Africa. From 2002 to 2005, he was a Research Associate with the German Advisory Council on Global Change WBGU. From 2005 to 2008, he was the Head of the Fuel Cell Systems Research Group, Fraunhofer Institute for Solar Energy Systems. Since 2008, he has been a Full Professor with the University of Oldenburg and the Director of the DLR Institute of Networked Energy Systems, until 2017 known as the NEXT ENERGY Institute. His research interests include materials and device development for energy converters, research into electrical energy technologies and systems and energy systems analysis.

...